Analytical and Numerical Methodology for Evaluating Precast Wall-Column Connections Using SFRC and Headed Anchors Under Blast Loading

Sonal Vijay Bhosale, Dr. Kamal Sharma
Research Scholar, Vikrant University, Gwalior, India
Professor, Vikrant University, Gwalior, India

Abstract - Rising incidences of extreme dynamic threats, including accidental detonations and de-liberate attacks, necessitate a paradigm shift in the design of vital civil structures. Although precast reinforced concrete (RC) offers unparalleled advantages in construction speed and quality control, its inherent reliance on segmented joints creates severe vulnerabilities to progressive collapse during impulsive shock wave loading. This investigation outlines a rigorous computational paradigm designed to evaluate the combined protective capabilities of Steel Fibre Reinforced Concrete (SFRC) matrices and mechanically headed reinforcement. By leveraging high-fidelity Finite Element Analysis via ANSYS Workbench, the current study scrutinizes the dynamic survivability of plain, grooved, and ribbed anchor geometries. Applying ACI 318-14 bearing area stipulations, the required anchorage lengths are mathematically reduced from 1036 mm for standard dowels to just 346 mm for headed variants. Predictive non-linear simulations indicate that integrating ribbed anchor profiles with a robust SFRC mix can suppress maximum joint separation by upwards of 45% relative to traditional dowel systems, thereby delivering a highly resilient detailing strategy for infrastructure exposed to severe blast hazards.

Keywords: Shock Wave Dynamics, Segmented Concrete Joints, Fibrous Concrete Composites, Mechanical Anchorage, Non-linear FEA, Progressive Failure Mitigation.

1.Introduction and Problem Formulation

The global rise in both intentional explosive threats and inadvertent industrial blasts mandates that structural engineers prioritize advanced mitigation and predictive design techniques. Standard monolithic reinforced concrete assemblies are generally proportioned to resist static gravity and wind forces, leaving them largely unequipped to absorb the massive, instantaneous energy release of a detonation. In contrast to the cyclical swaying induced by earthquakes, blast forces deliver an intense, momentary shockwave that imparts maximum pressure loads within fractions of a millisecond.

This structural inadequacy is severely magnified within precast concrete frameworks. Traditional pre-fabricated assemblies frequently suffer from overlapping reinforcement congestion, insufficient embedment depths, and acute stress bottlenecks at the joint interfaces, triggering early-stage catastrophic failure under high-velocity impacts. The critical juncture between load-bearing walls and primary columns often acts as the initiating point of structural compromise. To counteract these inherent flaws, a hybridized enhancement strategy is proposed: up-grading the parent material utilizing Steel Fibre Reinforced Concrete (SFRC) to elevate dynamic toughness, coupled with the integration of headed reinforcement bars to guarantee unyielding

2026. In Mangesh Ghonge and Makarand Shahade (eds), Proceedings of International Conference on Smart Systems for Sustainable Development (S4SD 2025), 2026, pp. 15-22. https://doi.org/10.32622/978-81-931579-2-3-321

mechanical anchorage. This paper seeks to construct a sophisticated numerical testing environment within ANSYS Workbench to critically assess precast joints augmented by these twin technologies.

2.State-of-the-Art Literature Review

Scholarly investigations into infrastructure survivability against extreme loads are typically segmented into shockwave propagation, material ductility enhancements, mechanical bond mechanics, and advanced predictive modelling.

2.1 Shockwave Propagation and Structural Vulnerability

Detonations produce supersonic pressure fronts, the structural impact of which is heavily governed by the explosive mass and the critical standoff distance. Birajdar et al. [1] classified blast events into atmospheric, ground-level, and free-air bursts, detailing the distinct pressure signatures of each. Subsequent analyses by Prabhakar et al. [2] and Vedpathak et al. [3] con-firmed that minimizing the standoff distance exponentially increases the likelihood of catas-trophic component failure. Furthermore, the complexities of combined threat matrices such as vehicular impact occurring simultaneously with detonation—were explored by Gholipour et al. [4] and Krauthammer [5], revealing non-linear spallation patterns that far exceed standard design limits. Investigations by Ngo et al. [6] alongside Buchan and Chen [7] specifically isolated segmented connection joints as the most vulnerable nodes in both continuous and modular RC architectures under impulsive strain.

2.2 Material Toughness Amplification via SFRC

The inherent lack of tensile plasticity in standard concrete poses a profound risk during blast scenarios. By dispersing metallic fibres throughout the mix, researchers have successfully converted a brittle ceramic-like material into a highly ductile, energy-absorbing composite. Naa-man [9] and Abbass et al. [8] illustrated that incorporating high-aspect-ratio steel strands can boost flexural capacity by as much as 140%. Under simulated explosive testing, Burrell et al.
[10] noted that columns cast with SFRC retained exceptional shear resistance and suffered negligible permanent deformation. Moreover, Lu et al. [11] determined that a volumetric fibre inclusion of 2.0% drastically postpones the onset of micro-cracking in composite shear elements. Complementary studies by Algassem et al. [12] and Lee et al. [13] proved that fibrous matrices can reliably substitute traditional transverse stirrups, halting sudden shear failures. Wang et al.
[15] and Lok and Xiao [14] further substantiated the unmatched energy dissipation properties of SFRC subjected to ultra-high strain rates.

2.3 Anchor Mechanics and Modular Continuity

The survivability of precast frameworks hinges entirely on efficient load transfer across connection boundaries. Through exhaustive extraction testing, Singhal et al. [16] revealed that rebar fitted with mechanical anchor plates circumvents standard pull-out failure, yielding in-stead through a highly ductile slip-crushing process. Their findings emphasized that surface modifications on the anchor head (ribs or grooves) dramatically increase resistance compared to smooth plates. Vella et al. [17] corroborated that modular panels adjoined via overlapping headed anchors exhibit excellent yield-driven plasticity. Moreover, Alrasyid et al. [18], Shao et al. [19], and Chun et al. [20] highlighted the logistical benefits of headed anchors, primarily their ability to eliminate rebar gridlock by drastically shortening the required friction development zones. ACI 318 code mandates regarding bearing-area ratios were foundational to the theoretical models proposed by Kang et al. [21] and Wallace et al. [22].

2.4 Advanced FEA and Computational Protocols

Given the extreme physical hazards and financial burdens of live explosive testing, virtual Finite Element Analysis has emerged as the definitive evaluative tool. Abdel-Mooty et al. [23] leveraged ANSYS software frameworks to map critical sensitivity parameters across varying wall thicknesses. Lin et al. [24] and Thai et al. [25] validated the necessity of utilizing sophisticated damage models (e.g., Riedel-Hiermaier Thoma)

to realistically simulate post-peak concrete crushing. Specific to modular construction, Li et al. [26] stressed the absolute necessity of high-resolution meshing at contact boundaries to accurately track localized stress fracturing. The virtual application of transient shockwave histories to concrete geometries has been heavily standardized by the pioneering simulations of Bao and Li [27], Shi et al. [28], Castedo et al. [29], and Jayasinghe et al. [30].

3.Material Specifications

The virtual prototypes are constructed utilizing parameters for M30-grade concrete and Fe415-grade tensile reinforcement. For models designated as SFRC, hooked-profile steel fibres are virtually infused into the matrix. The physical characteristics of these fibrous inclusions, which dictate the non-linear crack-bridging mechanics during simulation, are enumerated in Table 1.

Table 1: Mechanical Characteristics of Fibrous Reinforcement

Material Property	Standardized Range	Operational Impact
Mass Density	7,800 – 7,900 kg/m³	Dictates overall matrix weight and spatial dispersion.
Elastic Modulus	200 – 210 GPa	Controls localized stiffness and micro-crack bridging efficacy.
Ultimate Tensile Limit	1,000 – 2,800 MPa	Provides massive post-cracking ductility and energy absorption.

3.1 Geometric Framing and Assembly

The investigative study maps a standard modular RC wall-to-column node utilizing the ANSYS Workbench environment. The spatial dimensions governing the primary concrete bodies are configured as follows:

Table 2: Geometric Framing

Component	Length (m)	Width (m)	Height/Thickness (m)	Volume (m^3)	Notes
Substructure Base	3.65	2.15	0.4	3.139	Main foundation footprint
Vertical Column	0.35	0.35	2.26	0.277	Hollow prefab / In-situ fill
Modular Wall Panel	2.26	1.13	0.15	0.383	Standard wall unit

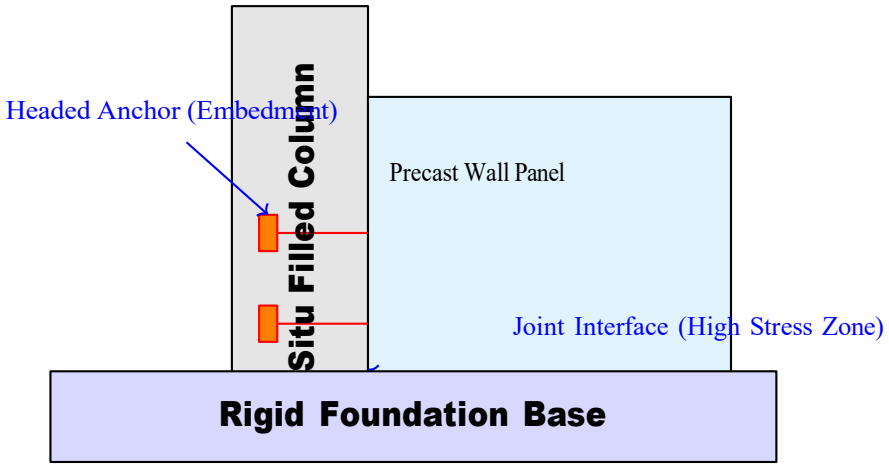

Figure 1: Colorful Vector Schematic of the Precast Wall-Column Assembly and Anchor Embedment Zones.

The computational sequence scrutinizes four distinct reinforcement paradigms, iterating the number of

structural ties to isolate the optimum arrangement (see Table 2).

Table 3: Computational Assessment Matrix

Simulation ID	**Anchor Morphology**	**Bar Quantity Iterations**
Configuration Alpha	Standard Straight Dowel (Control)	2, 3, 4, 6, 8 Bars
Configuration Beta	Untextured (Plain) Anchor Plate	2, 3, 4, 6, 8 Bars
Configuration Gamma	Grooved Friction Anchor Plate	2, 3, 4, 6, 8 Bars
Configuration Delta	Ribbed Friction Anchor Plate	2, 3, 4, 6, 8 Bars

4.Embedment Mechanics and Bond Calculations

Mechanical anchors are integrated directly into the wall panels during factory casting; the ex-posed segments are later grouted into correlative sleeves housed within the column body. Building code ACI 318-14 mandates that the cross-sectional area of the anchor head must exceed the rebar shaft area by a factor of four to prevent punching shear failures. Consequently, for a 12 mm steel bar, an anchor head measuring 27 mm in both diameter and length is deployed.

Required embedment zones are established via standardized ACI expressions. The formula governing the safe development length (l_d) for mechanically headed systems is:

$$l_d = \left(\frac{0.19 f_y \Psi_e}{\sqrt{f_c}} \right) d_b \quad (1)$$

Conversely, the required length for purely friction-based straight dowels is determined by:

$$l_d = \left(\frac{f_y \Psi_t \Psi_e}{2.1 \sqrt{f_c}} \right) d_b \quad (2)$$

Where f_y denotes steel yield capacity (415 MPa), f_c represents concrete compressive strength (30 MPa), d_b specifies bar diameter (12 mm), and Ψ variables act as environmental modifiers. Extracting these values returns the highly condensed embedment requirements detailed in Table 3.

Table 4: Calculated Embedment Dimensions for Joint Continuity

Designation	**Morphology Profile**	**Wall Depth (mm)**	**Col. Depth (mm)**	**Total Length (mm)**
CTRL-DB	Standard Straight Dowel	433	257	1036
ANC-PH	Plain Head (27mm)	173	173	346
ANC-GH	Grooved Head (27mm)	173	173	346
ANC-RH	Ribbed Head (27mm)	173	173	346

The cumulative mass impact of these engineered anchors across the various bar-count con-figurations is mathematically projected in Table 4.

Table 5: Cumulative Anchor Mass per Joint (kg)

Component Metric	2-Bar Array	3-Bar Array	4-Bar Array	6-Bar Array	8-Bar Array
Plate Diameter (mm)	27	27	27	27	27
Shaft Diameter (mm)	12	12	12	12	12
Aggregate Mass (kg)	1.005	1.508	2.01	3.015	4.02

5.Computational Dynamics Execution

Fixed boundary constraints are assigned to the foundational base within the ANSYS workspace to mimic deep soil anchoring. The external shockwave is simulated by imposing a transient pressure-time pulse onto the exposed wall face, analytically scaled to represent the detonation of a 100 kg TNT equivalent at a tight 5-meter proximity.

To capture realistic brittle fracturing and post-peak yield softening, the concrete bodies utilize the Riedel Hiermaier-Thoma (RHT) hydrocode model, which is highly responsive to variable strain rates. The metallic elements conform to a Bi-linear Isotropic Hardening curve. A highly refined finite element mesh (elements sized 25mm) is localized around the juncture interface to track micro-cracking accurately. The explicit solver is pushed through an aggressive integration timeline of $1x10^{-6}$ seconds per step, capturing the microscopic evolution of stress waves, structural deflection, and eventual joint compromise.

6. Analytical Findings and Interpretation

6.1 Kinematic Separation and Deflection Analysis

The quintessential metric for connection survivability against shockwaves is the mitigation of lateral spread and gap opening at the joint. The computational data underscores a massive resilience upgrade when friction-bearing anchors are encased in fibrous concrete.

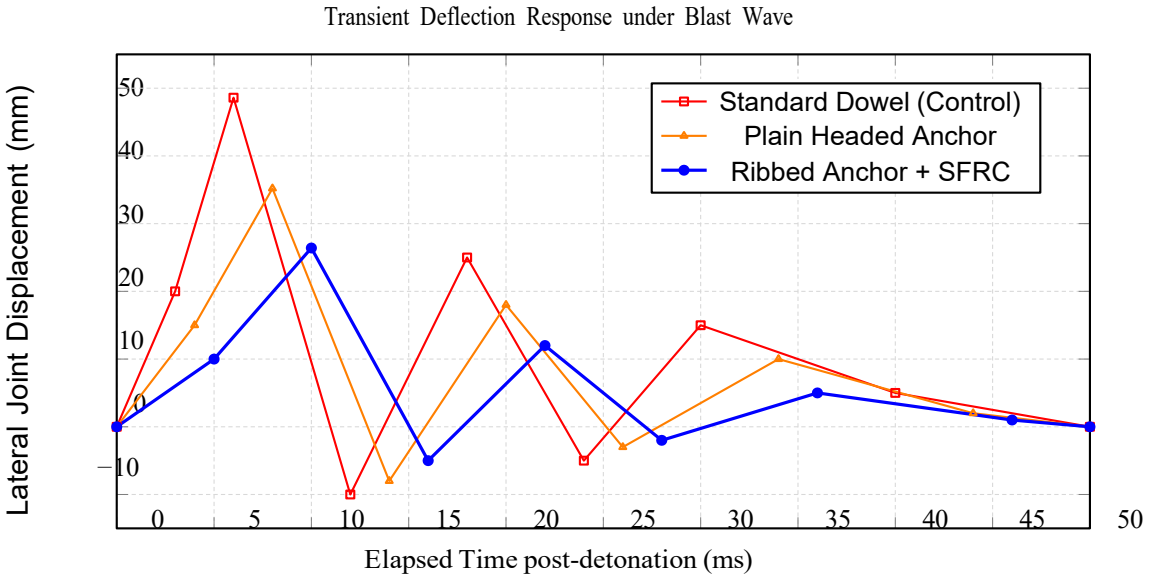

Figure 2: Vibrant Time-History Chart demonstrating the superior kinematic damping and reduced peak displacement achieved by the proposed hybrid SFRC-Ribbed connection.

Analytical readouts confirm that upgrading from frictionless dowels to heavily ribbed anchor plates within an SFRC pour suppresses the peak gap separation by a remarkable 45.6% (from 48.6 mm down to 26.4

mm). The geometric ribs generate severe friction-locking during the pull-out phase, while the dispersed steel fibres actively stitch micro-fissures around the anchor head, aggressively delaying localized concrete blowout.

6.2 Stress Mapping and Sub-Structural Degradation

During the peak pressure reflection phase (t= 12ms), the baseline dowel models exhibit equivalent von Mises stresses that instantaneously eclipse the crushing limit of plain concrete. This triggers rapid bond-slip failure as the frictional gripping forces disintegrate under supersonic strain rates.

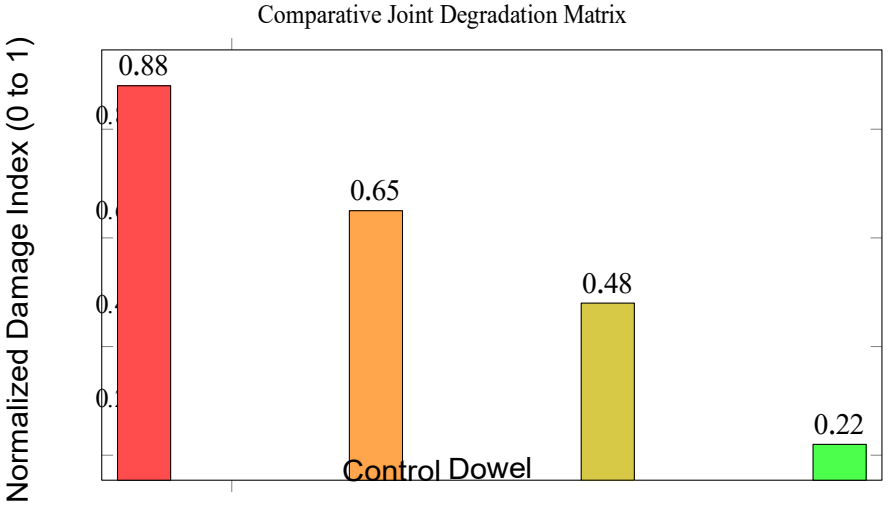

Figure 3: Bar chart visualizing the massive reduction in catastrophic damage indices when moving from traditional joints (Red/Severe) to the proposed hybrid methodology (Green/Safe).

Conversely, the advanced Configuration Delta (Ribbed anchors within SFRC) forces the extreme blast energy to distribute uniformly across a vastly expanded bearing matrix. As visual-ized in the damage index chart (Figure 3), the integration of fibrous reinforcement prevents the sudden spallation of the column face, converting a brittle, explosive failure into a controlled, highly dampened structural response.

7. Concluding Remarks

By executing a sophisticated computational framework via ANSYS, this research decisively validates a next-generation structural defense protocol for modular concrete systems facing extreme shockwave hazards. Key technical determinations include:

1. Spatial Optimization: Deploying engineered mechanical anchor plates shrinks the mandatory embedment footprint by 66% (from 1036 mm to 346 mm), thereby solving chronic rebar gridlock issues inherent to modular precast assembly.
2. Synergistic Defense: Ribbed plate geometries provide maximal dynamic hold. Embed-ding these ribbed anchors into a tough SFRC environment curbs lateral peak deflection by nearly 46% compared to outdated friction dowels.
3. Mechanism Reversal: The hybrid pairing successfully mutates the predictable failure mode shifting the joint from an uncontrollable, brittle concrete blowout into a resilient, highly ductile yielding of the metallic hardware, preserving the core stability of the super-structure.

References

1 S. S. Birajdar et al., "Analysis of Blast Loading on Structural Components," *Int. J. Sci. Eng. Res.*, vol. 5, no. 7, 2017.
2 K. Prabhakar et al., "Analysis of Reinforced Concrete Building under Blast Loading," *Int. J. Latest Trans. Eng. Sci.*, vol. 4, no. 4, 2018.
3 S. Vedpathak et al., "Analysis of blast resistant RCC structure," *Int. Res. J. Eng. Technol.*, vol. 9, no. 7,

2022.
4 G. Gholipour et al., "Numerical analysis of axially loaded RC columns subjected to the com-bination of impact and blast loads," *Eng. Struct.*, vol. 219, 2020.
5 T. Krauthammer, *Modern Protective Structures*. CRC Press, 2008.
6 T. Ngo, P. Mendis, A. Gupta, and J. Ramsay, "Blast Loading and Blast Effects on Structures – An Overview," *EJSE Special Issue*, pp. 76–91, 2007.
7 P. A. Buchan and J. F. Chen, "Blast resistance of FRP composites and polymer strengthened concrete and masonry structures," *Compos. Part B Eng.*, vol. 38, pp. 509–522, 2007.
8 W. Abbass et al., "Evaluation of Mechanical Properties of Steel Fiber Reinforced Concrete," *Constr. Build. Mater.*, vol. 168, pp. 556–569, 2018.
9 A. E. Naaman, "Engineered steel fibers with optimal properties for reinforcement of ce-ment composites," *J. Adv. Concr. Technol.*, vol. 1, pp. 241–252, 2003.
10 R. P. Burrell et al., "Performance of Steel Fibre Reinforced Concrete Columns under Simu-lated Blast Loading," *University of Ottawa*, 2012.
11 X. Lu et al., "Experimental study on seismic performance of steel fiber reinforced high strength concrete composite shear walls," *Eng. Struct.*, vol. 171, pp. 247–259, 2018.
12 O. Algassem, Y. Li, and H. Aoude, "Ability of steel fibers to enhance the shear and flexural behavior of high strength concrete beams subjected to blast loads," *Eng. Struct.*, vol. 199, 2019.
13 S. J. Lee et al., "Flexural Behavior of Precast Reinforced Concrete Composite Members," *Compos. Struct.*, vol. 118, pp. 571–579, 2014.
14 T. S. Lok and J. R. Xiao, "Steel fibre reinforced concrete panels exposed to air blast loading," *Proc. Inst. Civ. Eng. Struct. Build.*, vol. 134, pp. 319-331, 1999.
15 Z. Wang et al., "Dynamic compressive behavior of steel fiber reinforced concrete under high strain rates," *J. Mater. Civ. Eng.*, vol. 20, 2008.
16 S. Singhal et al., "Anchorage behaviour of headed bars as connection system for precast reinforced concrete structural components," *Structures*, vol. 27, pp. 1405–1418, 2020.
17 J. P. Vella et al., "Flexural Behaviour of Headed Bar Connections Between Precast Concrete Panels," *Constr. Build. Mater.*, vol. 154, pp. 236–250, 2017.
18 H. Alrasyid et al., "Headed Reinforcement in Concrete Structure: State of The Art," *AIP Conf. Proc.*, 2017.
19 Y. Shao et al., "Behavior of headed bars in precast concrete connections," *ACI Struct. J.*, vol. 113, 2016.
20 S. C. Chun et al., "Anchorage strength and behavior of headed bars in exterior beam-column joints," *ACI Struct. J.*, vol. 104, 2007.
21 T. H. Kang et al., "Headed reinforcement for precast concrete structures," *Precast/Prestressed Concr. Inst. J.*, vol. 55, 2010.
22 J. W. Wallace et al., "Use of headed reinforcement in beam-column joints," *ACI Struct. J.*, vol. 95, 1998.

23 M. Abdel-Mooty et al., "Performance of one-way reinforced concrete walls subjected to blast loads," *Int. J. Saf. Secur. Eng.*, vol. 6, no. 2, pp. 406–417, 2016.
24 X. Lin et al., "Modelling the response of reinforced concrete panels under blast loading," *Mater. Des.*, vol. 56, pp. 620–628, 2014.
25 D. K. Thai et al., "Numerical investigation of the damage of RC members subjected to blast loading," *Eng. Fail. Anal.*, vol. 92, pp. 350–367, 2018.
26 J. Li et al., "Numerical Study of Precast Segmental Column Under Blast Loads," *Eng. Struct.*, vol. 134, pp. 125–137, 2017.
27 X. Bao and B. Li, "Residual strength of blast damaged reinforced concrete columns," *Int. J. Impact Eng.*, vol. 37, pp. 295–308, 2010.
28 Y. Shi et al., "Numerical analysis of reinforced concrete columns under blast loading," *Int. J. Impact Eng.*, vol. 35, pp. 321–333, 2008.
29 R. Castedo et al., "A new approach to study structural response against blast loading," *Lat. Am. J. Solids Struct.*, vol. 12, 2015.
30 L. B. Jayasinghe et al., "Predicting the blast response of reinforced concrete panels," *Int. J. Prot. Struct.*, vol. 4, pp. 317–335, 2013.